

Numerical calculation of electron density distribution in modulation-doped GaAs/AlGaAs heterostructures

MICHAŁ SZYMAŃSKI, MARIUSZ ZBROSZCZYK

Institute of Electron Technology, al. Lotników 32/46, 02-668 Warszawa, Poland.

Electron density distribution in GaAs/AlGaAs heterostructure is calculated. In addition, the diagram of the conduction band edge is presented. The results were obtained through the self-consistent solution of one-dimensional Schrödinger–Poisson equations. For numerical calculations the finite-difference method with non-uniform mesh has been used.

1. Introduction

Recent, dynamic development of such techniques like molecular beam epitaxy or metal-organic chemical vapour deposition enables growth of low-dimensional, multi-layer, modulation-doped semiconductor structures of excellent uniformity. These structures are used for producing different opto- and microelectronic devices like lasers, detectors or transistors. However, understanding their optical and transport properties requires the self-consistent solution of both Schrödinger and Poisson equations. For example, such a solution enables the calculations of material gain in the active layer of a laser [1], density of two-dimensional electron gas in high-electron-mobility transistor (HEMT) [2] or interpretation of the inverse capacitance-voltage profiling technique [3].

In this work we create software for finding a self-consistent solution of one-dimensional Schrödinger–Poisson equations. Next, we apply our numerical tools for investigating the n-doped GaAs/AlGaAs heterostructure of HEMT grown in molecular beam epitaxy (MBE) reactor in Institute of Electron Technology, Warsaw, Poland. As a result we present electron density and conduction band edge versus spatial coordinate. Our software is based on the finite-difference method. Because of the large differences between layer thicknesses we decided to use a non-uniform mesh.

2. Basic equations

The one-dimensional, one-electron Schrödinger equation is

$$-\frac{\hbar^2}{2} \frac{d}{dx} \left(\frac{1}{m_{\text{eff}}(x)} \frac{d}{dx} \psi(x) \right) + V(x) \psi(x) = E \psi(x) \quad (1)$$

where ψ is the wave function, E is the energy, V is the potential energy, \hbar is the Planck constant divided by 2π and m_{eff} is the electron effective mass. The one-dimensional Poisson equation is

$$\frac{d}{dx} \left(\epsilon_s(x) \frac{d}{dx} \right) \phi(x) = -\frac{q}{\epsilon_0} (N_D(x) - n(x)) \quad (2)$$

where ϵ_s is the dielectric constant, ϕ is the electrostatic potential, N_D is the ionized donor concentration and n is the electron density distribution. Electron distribution in the conduction band can be found when the potential energy V is set to be equal to the conduction-band edge energy [4]. The potential energy V is related to the electrostatic potential ϕ as follows [4]:

$$V(x) = -q\phi + \Delta E_c(x) \quad (3)$$

where ΔE_c is the pseudopotential energy due to the band offset at the heterointerface. The wave function ψ and electron density n are related by

$$n(x) = \sum_{k=1}^m \psi^*(x) \psi(x) n_k \quad (4)$$

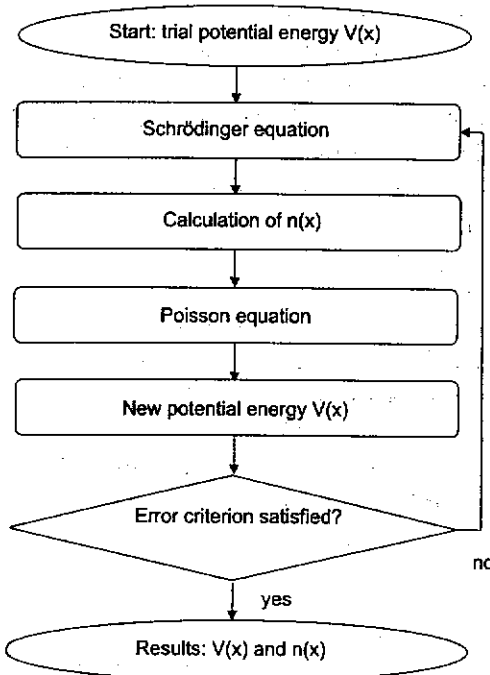


Fig. 1. Iteration scheme for finding the self-consistent solution of one-dimensional Schrödinger-Poisson equations.

where m is the number of bound states, n_k is electron occupation of k -th state of energy E_k and is expressed by

$$n_k = \frac{m_{\text{eff}}}{\pi \hbar^2} \int_{E_k}^{\infty} \frac{1}{1 + \exp\left(\frac{E - E_F}{kT}\right)} dE. \quad (5)$$

Self-consistent solutions of Eqs. (1) and (2) are obtained through the iteration procedure symbolically depicted by block diagram in Fig. 1. The error criteria are defined as changes δV and δn smaller than arbitrary assumed values.

3. Numerical methods

In order to solve Eqs. (1) and (2) we used the finite-difference method. Since the analyzed semiconductor structures contain layers of significantly different thicknesses, many parameters may vary rapidly in some regions and slowly in other. Thus, we decided to use a non-uniform mesh (see Fig. 2) and wrote three-point approximation of the function derivative as

$$\frac{df(x_j)}{dx} \approx \frac{f\left(x_j + \frac{1}{2}h_{j+1}\right) - f\left(x_j - \frac{1}{2}h_{j+1}\right)}{\frac{1}{2}h_{j+1} + \frac{1}{2}h_j}. \quad (6)$$

In Equation (6) half-steps have been used deliberately. Schrödinger (Poisson) equation relates the wave function (electrostatic potential) with its second derivative. Thus, after discretization, values of ψ and ϕ in mesh points only have been required.

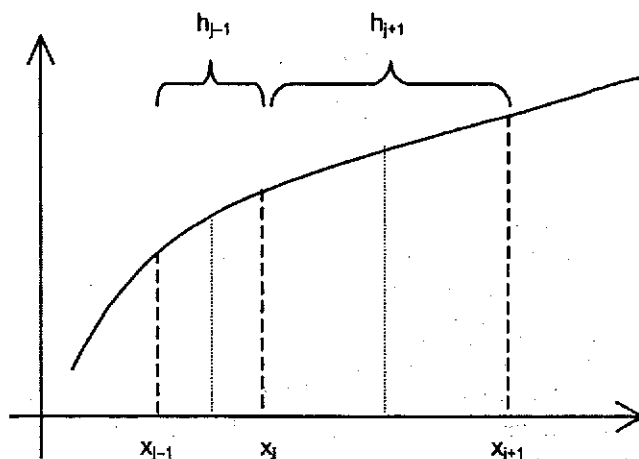


Fig. 2. Discretization of ψ or ϕ using a non-uniform mesh.

Using the rule (6) to Schrödinger equation (Eq. (1)) we get a set of N linear equations, where N is the total number of mesh points. Therefore, the discrete form of Eq. (1) may be written as $N \times N$ matrix equation

$$\sum_{j=1}^N A_{ij} \psi_j = E \psi_i \quad (7)$$

where

$$A_{ij} = \begin{cases} \frac{\hbar^2}{2 m_{j+1/2} h_{j+1} (h_{j+1} + h_j)}, & j = i+1, \\ \frac{\hbar^2}{2 m_{j-1/2} h_j (h_{j+1} + h_j)}, & j = i-1, \\ -A_{i,i+1} - A_{i,i-1} + V_i, & j = i, \\ 0, & \text{in remaining cases} \end{cases} \quad (8)$$

Diagonalization of matrix A allows to find bound states for a particular profile $V(x)$.

Application of rule (6) to Poisson equation (Eq. (2)) leads to $N \times N$ non-linear set of equations:

$$F_i(\varphi_1, \varphi_2, \dots, \varphi_N) = 0 \quad (9)$$

where φ_i is the value of the electrostatic potential in the i -th point of the mesh and the i -th equation takes the form

$$\frac{2}{h_i(h_{i+1} + h_i)} \varphi_{i-1} - \frac{2}{h_i h_{i+1}} \varphi_i + \frac{2}{h_{i+1}(h_{i+1} + h_i)} \varphi_{i+1} + \frac{e}{\epsilon_s} (N_{D,i} - n_i) = 0. \quad (10)$$

Solution of Eq. (10) is found by Newton-Raphson method [5].

4. Results and discussion

Quasi-one-dimensional GaAs/AlGaAs heterostructures tend to have conduction band edge exhibiting several quantum wells where bound states may appear. Consequently in all these wells electrons may be accumulated. However, the proper operation of most semiconductor devices requires high electron concentration in a very small region. Particularly, in investigation of HEMTs, one of the most important subjects has been the improvement of two-dimensional electron gas concentration [6]. An example of the well-designed heterostructure one can find in paper [4] where electrons are confined to one region, namely at the interface of AlGaAs quantum well and undoped GaAs layer.

Numeri

Mate

GaAs

Al_{0.3}GAl_{0.3}G

GaAs

GaAs

Fig. 3. S

600

Energy [meV]

300

0

0

Fig. 4. R

In t
in Fig.
the dop
differ s
conduc
of the r

linear
form of

(7)

(8)

$V(x)$.
ear set

(9)

nd the

(10)

band
uently
ion of
small
bjects
)]. An
ctrons
ll and

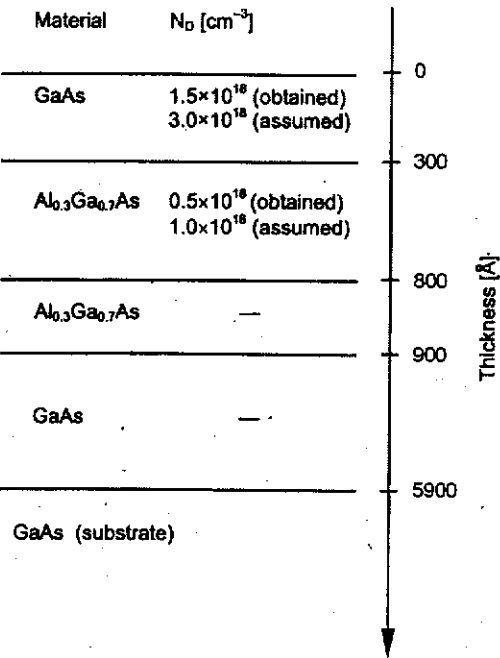


Fig. 3. Schematic view of the investigated heterostructure.

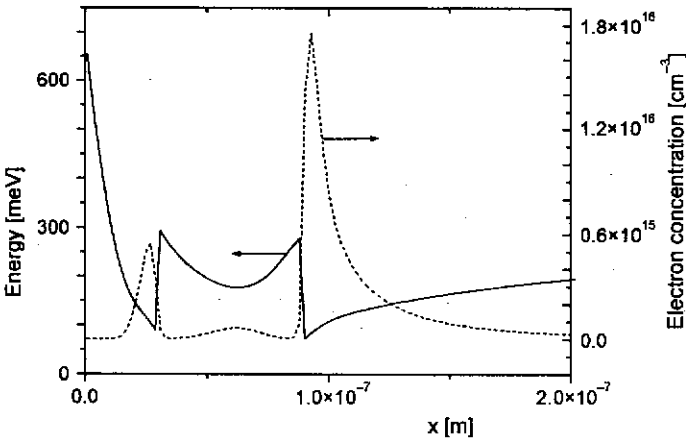


Fig. 4. Results for the obtained concentration.

In this work we consider a GaAs/AlGaAs heterostructure schematically depicted in Fig. 3. It has been grown by MBE in Institute of Electron Technology. Note that the doping concentrations assumed and obtained during the technological process differ significantly. For both cases we calculated the electron concentration $n(x)$ and conduction band edge $V(x)$. The diagrams are presented in Figs. 4 and 5. In the case of the real heterostructure (Fig. 4) we see the undesired three-peak profile of electron

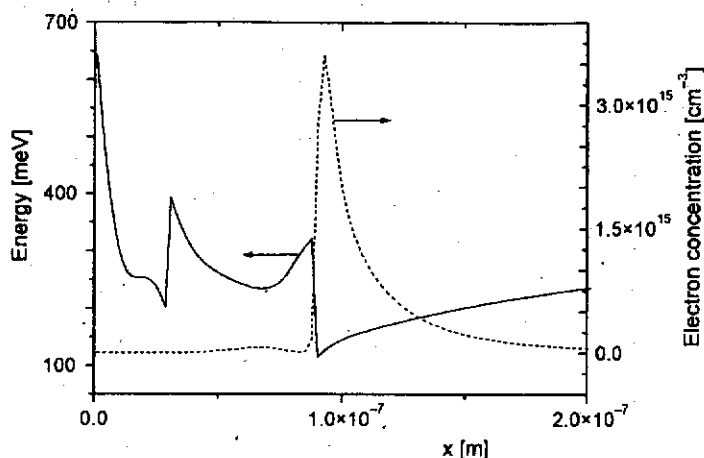


Fig. 5. Results for the assumed concentration.

concentration. This indicates that a large part of electrons has been accumulated in three regions: at the doped GaAs–doped AlGaAs interface, in AlGaAs layers and at the undoped AlGaAs–undoped GaAs interface. Calculations done for the assumed doping profile (Fig. 5) show that almost all the electrons are confined at the undoped AlGaAs–undoped GaAs interface. Thus the deviations of doping profile, occurring during technological processes, may significantly influence the features of heterostructures.

References

- [1] CHUANG S.L., *Physics of Optoelectronics Devices*, Wiley, New York, Chichester 1995.
- [2] BOUZAIENE L., SFAXI L., MAAREF H., *Microelectron. J.* **30** (1999), 705.
- [3] KIKUCHI N., OGAWA M., MIYOSHI T., *Solid-State Electron.* **44** (2000), 1663.
- [4] TAN I-H., SNIDER G.L., CHANG L.D., HU E.L., *J. Appl. Phys.* **68** (1990), 4071.
- [5] PRESS W.H., TEUKOLSKY S.A., VETTERLING W.T., FLANNERY B.P., *Numerical Recipes in FORTRAN*, Cambridge University Press, Cambridge 1992.
- [6] BOUZAIENE L., SFAXI L., SGHAEIR H., MAAREF H., *J. Appl. Phys.* **85** (1999), 8223.

Received May 13, 2002